

A mixed metal phosphate incorporating isonicotinate ligand: synthesis, crystal structure, and magnetic properties of $\text{Cu}(\text{HINT})(\text{VO}_2)(\text{PO}_4)$

Chih-Min Wang,^a Ya-Lan Chuang,^a Shiuan-Ting Chuang,^a and Kwang-Hwa Lii^{a,b,*}

^aDepartment of Chemistry, National Central University, Chungli, Taiwan 320, ROC

^bInstitute of Chemistry, Academia Sinica, Nankang, Taipei, Taiwan 115, ROC

Received 30 October 2003; received in revised form 12 January 2004; accepted 29 February 2004

Abstract

A mixed metal phosphate incorporating isonicotinate ligand, $\text{Cu}(\text{HINT})(\text{VO}_2)(\text{PO}_4)$, was hydrothermally synthesized and characterized by single-crystal X-ray diffraction and magnetic susceptibility. This compound crystallizes in the monoclinic space group $C2/c$ with cell parameters $a = 22.033(1) \text{ \AA}$, $b = 6.2986(3) \text{ \AA}$, $c = 16.0202(9) \text{ \AA}$, $\beta = 121.001(1)$, and $Z = 8$. The structure consists of two-dimensional neutral sheets of $\text{CuVO}_2(\text{PO}_4)$ with the dipolar isonicotinate ligand being coordinated to Cu ions as a pendent group. Adjacent sheets are connected by hydrogen bonding. Each sheet consists of infinite chains of CuO_6 octahedra sharing *trans* edges which are connected by double chains of vanadyl(V) phosphate via corner sharing. Magnetic study results indicate the presence of intrachain ferromagnetic coupling between Cu ions. The magnetic exchange parameter was estimated as $2J/k = 51.83 \text{ K}$ based on an $S = 1/2$ equally spaced ferromagnetic chain model.

© 2004 Elsevier Inc. All rights reserved.

Keywords: Phosphate; Isonicotinate; Copper; Vanadium

1. Introduction

Recently, many research activities have focused on the synthesis of organic–inorganic hybrid compounds by incorporating organic ligands in the structures of metal phosphates. The underlying idea is to combine the robustness of inorganic phosphate frameworks with the versatility and chemical flexibility of organic ligands. A large number of oxalate-phosphates and bipyridine-phosphates of transition metals and group 13 elements have been reported [1,2]. More recently, we have been interested in the synthesis of metal phosphates with the multifunctional organic ligand isonicotinate (abbreviated as INT) (4-pyridinecarboxylate) in which both neutral N-donor and anionic O-donor groups are present, because several coordination polymers based on INT ligand have shown interesting physical properties and structural chemistry [3,4]. We have synthesized

the first metal phosphate incorporating isonicotinate ligand, $\text{Zn}(\text{HINT})(\text{HPO}_4)$ [5]. Its structure consists of two-dimensional neutral sheets of $\text{Zn}(\text{HPO}_4)$ with the dipolar isonicotinate ligand being coordinated to zinc as a pendent group. ^1H MAS NMR spectroscopy showed the presence of a proton bonded to the pyridine nitrogen atom, which confirms the presence of $^+\text{HNC}_5\text{H}_4\text{COO}^-$. As part of continuing work of this system, a mixed metal phosphate incorporating isonicotinate ligand, $\text{Cu}(\text{HINT})(\text{VO}_2)(\text{PO}_4)$ (**1**) was synthesized. In this paper, the synthesis, crystal structure, and magnetic properties of the new compound are presented.

2. Experimental

2.1. Synthesis and initial characterization

The hydrothermal reactions were carried out in Teflon-lined stainless steel Parr acid digestion bombs. All chemicals were purchased from Aldrich. Reaction of V_2O_5 (0.25 mmol), $\text{Cu}(\text{NO}_3)_2 \cdot 3\text{H}_2\text{O}$ (0.5 mmol),

*Corresponding author. Institute of Chemistry Academia Sinica, National Central University, Chungli, Nankang, Taipei 320, Taiwan 320, ROC. Fax: +886-3-422-7664.

E-mail address: liikh@cc.ncu.edu.tw (K.-H. Lii).

isonicotinic acid (3 mmol), H_3PO_4 (3 mmol), and H_2O (10 mL) at 165°C for 3 days produced green tablet crystals of **1** as the major product and some orange solid. The products were filtered, washed with water, rinsed with ethanol, and dried in a desiccator. Attempts to prepare a pure product have been unsuccessful. The sample used for further studies were hence from manually selected crystals of which the X-ray powder diffraction pattern agreed well with that calculated from single-crystal data. Energy-dispersive X-ray fluorescence spectroscopy of several green crystals confirms the presence of Cu, V and P. Elemental analysis results are consistent with the stoichiometry (Found: C, 19.40; H, 1.44; N, 3.68%. Calcd for $\text{C}_6\text{H}_5\text{NO}_8\text{PCuV}$: C, 19.77; H, 1.38; N, 3.84%) (Fig. 1).

2.2. Single-crystal X-ray diffraction

A suitable crystal of **1** with dimensions $0.12 \times 0.1 \times 0.05$ mm was selected for indexing and intensity data collection on a Siemens SMART CCD diffractometer equipped with a normal focus, 3-kW sealed tube X-ray source. Intensity data were collected at room temperature in 1271 frames with ω scans (width 0.30° per frame). Empirical absorption corrections based on symmetry equivalents were applied ($T_{\text{min, max}} = 0.603, 0.927$). The structure was solved by direct methods and difference Fourier syntheses. The H atom bonded to the pyridine N atom was located in difference Fourier maps. The H atoms, which are

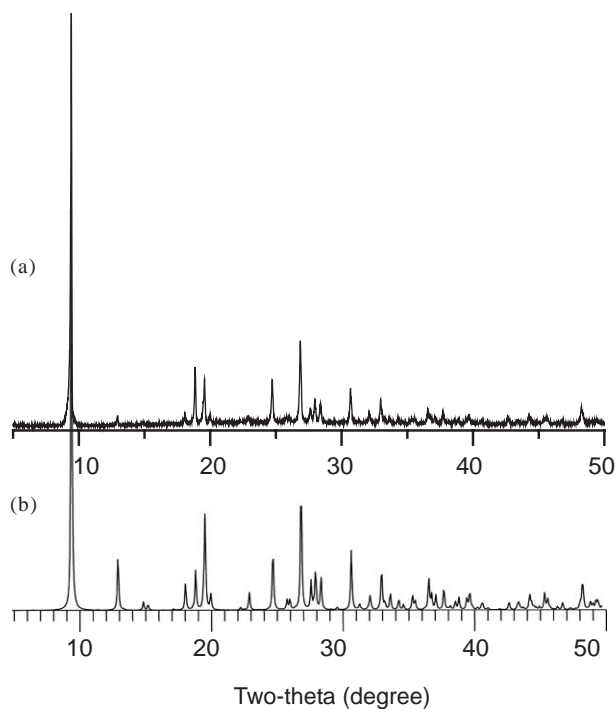


Fig. 1. Experimental X-ray powder pattern (top) and simulated powder pattern based on the results from single-crystal X-ray diffraction (bottom) for **1**.

bonded to C atoms, were positioned geometrically and refined using a riding model. The final cycles of least-squares refinement included atomic coordinates and anisotropic thermal parameters for all non-hydrogen atoms and a fixed isotropic thermal parameter for the pyridinium H atom. The final difference Fourier maps were flat ($\Delta\rho_{\text{max, min}} = 0.50, -0.51 \text{ e}/\text{\AA}^3$). All calculations were performed using the SHELXTL Version 5.1 software package [6]. CIF file for **1** has been deposited with the Cambridge Crystallographic Data Centre as supplementary publication no. CCDC-223134.

2.3. Magnetic susceptibility measurements

Variable-temperature magnetic susceptibility $\chi(T)$ data were obtained on 30.3 mg of polycrystalline sample of **1** from 2 to 300 K in a magnetic field of 2000 G after zero-field cooling using a SQUID magnetometer. The diamagnetic correction ($-149 \times 10^{-6} \text{ cm}^3/\text{mol}$) was made according to Selwood [7].

3. Results and discussion

3.1. Description of the structure

The crystal data and structure refinement parameters are given in Table 1, atomic coordinates in Table 2, and selected bond lengths in Table 3. All atoms are at general positions. On the basis of magnetic susceptibility study (vide infra), bond-valence calculations [8] and the presence of dioxovanadium unit, the Cu atom is divalent

Table 1
Crystallographic data for $\text{Cu}(\text{HINT})(\text{VO}_2)(\text{PO}_4)$

Formula	$\text{C}_6\text{H}_5\text{NO}_8\text{PVCu}$
M	364.56
Crystal system	Monoclinic
Space group	$C2/c$ (No. 15)
a (\AA)	22.033(1)
b (\AA)	6.2986(3)
c (\AA)	16.0202(9)
β (deg)	121.001(1)
V (\AA^3)	1905.7(3)
Z	8
T ($^\circ\text{C}$)	23
λ (MoK α) (\AA)	0.71073
D_{calc} (g/cm^3)	2.541
μ (MoK α) (cm^{-1})	34.2
Measured reflections	12302
Unique reflections (R_{int})	2273 (0.0315)
Observed reflections [$I > 2\sigma(I)$]	1963
R_1^a	0.0264
wR_2^b	0.0672

$$^a R_1 = \sum ||F_o| - |F_c|| / \sum |F_o|.$$

$$^b wR_2 = \sum \{ [w(F_o^2 - F_c^2)^2] / \sum [w(F_o^2)^2] \}^{1/2}, \quad w = 1 / [\sigma^2(F_o^2) + (aP)^2 + bP],$$

$$P = [\text{Max}(F_o, 0) + 2(F_c)^2] / 3, \quad \text{where } a = 0.0346 \text{ and } b = 2.03.$$

Table 2
Atomic coordinates and thermal parameters (\AA^2) for Cu(HINT)
(VO₂)(PO₄)^a

Atom	x	y	z	U_{eq}^b
Cu(1)	0.24849(1)	0.22875(4)	0.74470(2)	0.0126(1)
V(1)	0.33503(2)	-0.012261(6)	0.62939(3)	0.0102(1)
P(1)	0.28300(3)	0.49473(9)	0.60491(4)	0.0102(1)
O(1)	0.31349(9)	0.2850(2)	0.5975(1)	0.0162(4)
O(2)	0.34124(8)	0.6638(2)	0.6338(1)	0.0136(3)
O(3)	0.26677(9)	0.4836(2)	0.6884(1)	0.0133(4)
O(4)	0.21662(9)	0.5569(3)	0.5102(1)	0.0146(4)
O(5)	0.33374(9)	0.2963(3)	0.8677(1)	0.0200(4)
O(6)	0.16467(9)	0.1535(3)	0.6188(1)	0.0194(4)
O(7)	0.3140(1)	-0.0164(3)	0.7146(1)	0.0196(4)
O(8)	0.42035(9)	0.0090(2)	0.6817(1)	0.0184(4)
N(1)	0.5447(1)	0.4031(4)	0.1870(2)	0.0229(5)
H(1N)	0.582(2)	0.384(6)	0.245(3)	0.05
C(1)	0.3577(1)	0.4688(4)	-0.0897(2)	0.0144(5)
C(2)	0.4240(1)	0.4480(4)	0.0102(2)	0.0149(5)
C(3)	0.4572(1)	0.2529(4)	0.0395(2)	0.0210(6)
C(4)	0.5182(1)	0.2341(4)	0.1292(2)	0.0246(6)
C(5)	0.4525(1)	0.6211(1)	0.0723(2)	0.0196(5)
C(6)	0.5138(1)	0.5949(4)	0.1614(2)	0.0233(6)

^aThe H atoms which are bonded to C atoms are given in supplementary materials.

^b U_{eq} is defined as one-third of the trace of the orthogonalized U_{ij} tensor. The isotropic thermal parameter for H(1N) is fixed.

Table 3
Selected bond lengths, bond-valence sums and bond angles for
Cu(HINT)(VO₂)(PO₄)^a

Bond lengths (\AA) and bond-valence sums ($\sum s$)			
Cu(1)–O(3)	1.981(2)	Cu(1)–O(3) ⁱ	2.004(2)
Cu(1)–O(5)	1.944(2)	Cu(1)–O(6)	1.966(2)
Cu(1)–O(7)	2.327(2)	Cu(1)–O(7) ⁱⁱ	2.412(2)
$\sum s(\text{Cu(1)–O}) = 2.12$			
V(1)–O(1)	1.934(2)	V(1)–O(2) ⁱⁱⁱ	2.044(2)
V(1)–O(4)	1.937(2) ^{iv}	V(1)–O(7)	1.653(2)
V(1)–O(8)	1.622(2)		
$\sum s(\text{V(1)–O}) = 5.05$			
P(1)–O(1)	1.514(2)	P(1)–O(2)	1.544(2)
P(1)–O(3)	1.554(2)	P(1)–O(4)	1.520(2)
$\sum s(\text{P(1)–O}) = 5.03$			
N(1)–C(4)	1.332(4)	N(1)–C(6)	1.343(4)
N(1)–H(1N)	0.88(4)	C(1)–O(5) ^v	1.247(3)
C(1)–O(6) ^{vi}	1.256(3)	C(1)–C(2)	1.517(3)
C(2)–C(3)	1.383(3)	C(2)–C(5)	1.390(3)
C(3)–C(4)	1.378(4)	C(5)–C(6)	1.380(3)
Bond angles (deg)			
O(7)–Cu(1)–O(5)	88.65(7)	O(7)–Cu(1)–O(6)	89.01(7)
O(7)–Cu(1)–O(3)	98.65(6)	O(7)–Cu(1)–O(3) ⁱ	83.80(6)
O(7)–Cu(1)–O(7) ⁱⁱ	176.75(1)	Cu(1)–O(3)–Cu(1) ⁱⁱ	104.58(8)
Cu(1)–O(3)–P(1)	128.23(9)	Cu(1) ⁱⁱ –O(3)–P(1)	127.01(9)
Cu(1)–O(7)–Cu(1) ⁱ	83.38(6)		

Symmetry codes: (i) $-x + 1/2, y - 1/2, -z + 3/2$; (ii) $-x + 1/2, y + 1/2, -z + 3/2$; (iii) $x, y + 1/2, z$; (iv) $-x + 1/2, -y + 1/2, -z + 1$; (v) $x, y, z - 1$; (vi) $-x + 1/2, y + 1/2, -z + 1/2$.

^aThe C–H bond lengths are 0.93 \AA .

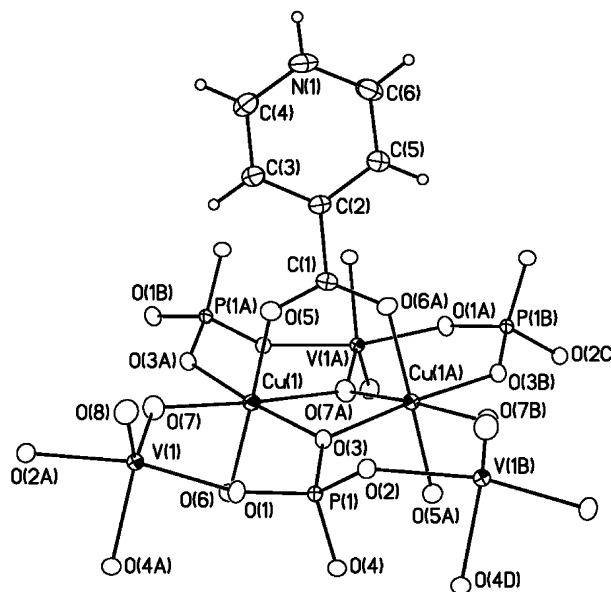


Fig. 2. The coordination environments of the metal atoms in the structure of **1** showing atom labeling scheme. Thermal ellipsoids are shown at 50% probability. Small open circles are H atoms.

and the V atom is pentavalent. Fig. 2 shows the coordination environments of Cu and V atoms and atom labeling scheme. The d^9 configuration makes Cu^{II} subject to Jahn–Teller distortion. The Cu atom is 6-coordinate in a geometry of octahedron elongated in one direction. There is a planar array of four short Cu–O bonds (1.944–2.004 \AA) formed by two phosphate and two carboxylate groups, and two very long Cu–O(7) bonds (2.327 and 2.412 \AA). Atom O(7) has a smaller ligand field strength and prefers the apical positions with stretched bonds because it forms a very short V–O distance corresponding to a vanadyl (V=O) group formed by $p\pi$ donation from oxygen to vacant $3d\pi$ -orbitals on vanadium. Each V⁵⁺ cation has a distorted trigonal bipyramidal coordination in which two equatorial positions are occupied by doubly bonded oxygen atoms (O(7) and O(8)) and the remaining positions are occupied by three PO₄³⁻ anions. Each phosphate ligand coordinates to two Cu and three V atoms. One of the oxygen atoms in the PO₄ group, O(3), connects two Cu atoms. The HINT ligand is a dipolar ion, namely the carboxylate group loses a proton, giving a carboxylate ion, and the pyridine nitrogen is protonated to a pyridinium ion. The pyridyl ring and carboxylate group are slightly twisted at an angle of 9.2°. Each carboxylate group is coordinated to two Cu ions.

The structure consists of two-dimensional neutral sheets of Cu(HINT)(VO₂)(PO₄) in the bc plane (Fig. 3). There are two sheets per unit cell length along the a -axis. Each sheet, shown in Fig. 4, is constructed from infinite chains of *trans*-edge-sharing CuO₆ octahedra running along the b -axis. The Cu ions within a chain are equally

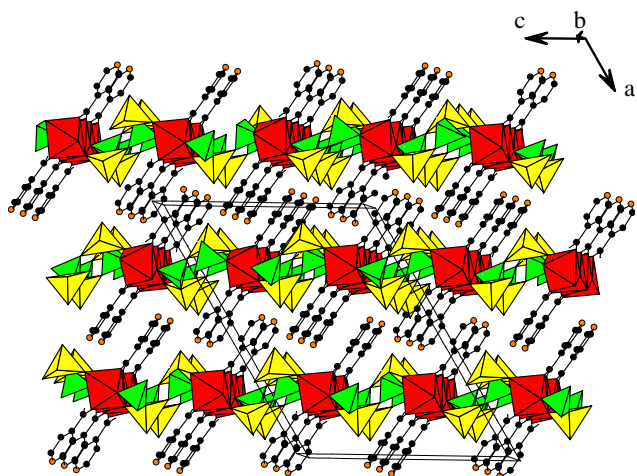


Fig. 3. Structure of **1** viewed approximately along the *b*-axis. The polyhedra with dark gray, light gray, and white patterns are CuO₆ octahedra, VO₅ trigonal bipyramids, and PO₄ tetrahedra, respectively. Black circles, C atoms; open circles, N atoms. H atoms are not shown.

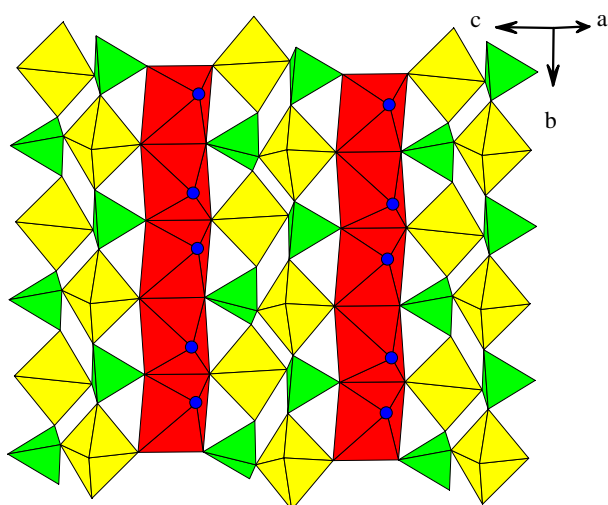


Fig. 4. Section of a metal phosphate layer in **1**. Open circles are the oxygen atoms of carboxylate groups in HINT ligands.

spaced with a distance of 3.153 Å. The VO₅ and PO₄ polyhedra alternate along the *b*-axis to form a chain in which each polyhedron shares an oxygen with one neighboring chain, leading to a double chain. Adjacent Cu chains are connected by double chains of vanadyl(V) phosphate via corner sharing. The carboxylate group of each HINT ligand coordinates to two neighboring Cu ions within a chain and the pyridinium group extends away from the layer into the interlamellar region. Neighboring HINT ligands from adjacent layers have a structure of offset parallel stacking and are separated by 3.34 Å, indicating significant π – π interaction. Therefore, the 2D layers of **1** are extended into a 3D

supramolecular array via the zipper-like interaction of the lateral aromatic groups. This structural feature is related to recently reported layer compounds [9]. There are hydrogen bonds between adjacent layers as indicated by the short H(1N)···O(2) distance of 1.82 Å and N(1)–H(1N)–O(2) bond angle of 178°.

3.2. Magnetic susceptibility

The inverse magnetic susceptibility, shown in Fig. 5, follows the equation $\chi = C/(T - \theta)$, and a linear fit for $T > 50$ K data gave a Weiss temperature $\theta = 13.6$ K and a Curie constant $C = 0.518$ cm³ K/mol. The positive θ value suggests an overall ferromagnetic interaction between Cu ions. From the equation, $C = N\mu_{\text{eff}}^2/3k_{\text{B}}$, one obtains the effective magnetic moment μ_{eff} per formula unit = 2.04 BM, which confirms the presence of one unpaired electron per formula unit and is consistent with the observation that the magnetic moments of Cu^{II} complexes are generally in the range from 1.75 to 2.20 BM. As shown in Fig. 5 the $\chi_{\text{M}}T$ value increases with decreasing temperature, indicating again that the main magnetic interaction between Cu ions is ferromagnetic. The experimental data were analyzed by an $S = 1/2$ ferromagnetic chain model with the Hamiltonian $H = -2J\sum S_i \cdot S_{i+1}$ using the following polynomial expression [10]:

$$\chi = (Ng^2\mu_{\text{B}}^2/4kT)(A/B)^{2/3} + \chi_{\text{TIP}},$$

where $A = 1.0 + 5.7979916y + 16.902653y^2 + 29.376885y^3 + 29.832959y^4 + 14.036918y^5$, $B = 1.0 + 2.7979916y + 7.0086780y^2 + 8.6538644y^3 + 4.5743114y^4$, $y = J/2kT$, χ_{TIP} = temperature independent paramagnetism, and other symbols have their usual meanings.

When the interchain interaction is taken into account:

$$\chi_{\text{m}} = \chi/[1 - \chi(2zj'/Ng^2\mu_{\text{B}}^2)],$$

where zj' represents the possible exchanges between Cu chains. The results of the best fit are shown in Fig. 5 for $g = 2.0844$, $2J/k = +51.83$ K, $2zj' = -0.0010$ K, $\chi_{\text{TIP}} = 0.00035$ cm³/mol, and the coefficient of determination (r^2) = 0.99751. The $2J/k$ value for **1** is comparable to that for [Cu(hfac)₂hin], which shows intrachain ferromagnetic coupling between copper and radical spins [11]. But the interchain interaction in **1** is considerably smaller (–0.0010 K vs. –0.91 K). The very weak interchain interaction in **1** can be ascribed to the long separation between neighboring Cu chains by double chains of vanadyl(V) phosphate. The ferromagnetic interaction can be interpreted as follows. Each Cu ion has 4 + 2 coordination because of Jahn–Teller effect. The magnetic orbital is $d_{x^2-y^2}$ orbital. As shown in Fig. 6, neighboring Cu ions are bridged by two oxygen atoms. The Cu–O(7)–Cu and Cu–O(3)–Cu bond angles are 83.38(6)° and 104.58(8)°, respectively. One of the bridging atoms, O(7), takes the positions with the

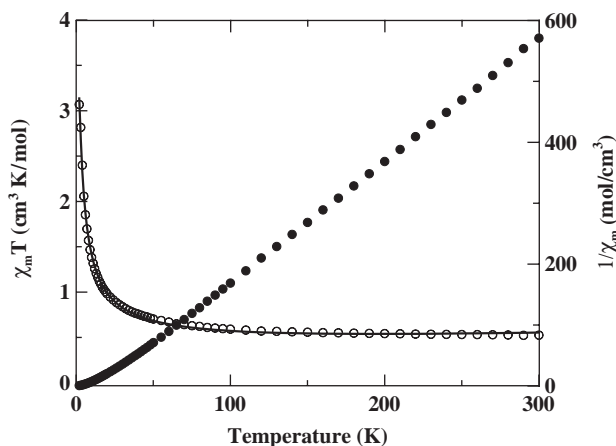


Fig. 5. Temperature dependence of $\chi_m T$ (open circles) and χ_m^{-1} (solid circles) for **1**. The solid line represents the theoretical curve based on an $S = 1/2$ ferromagnetic chain model.

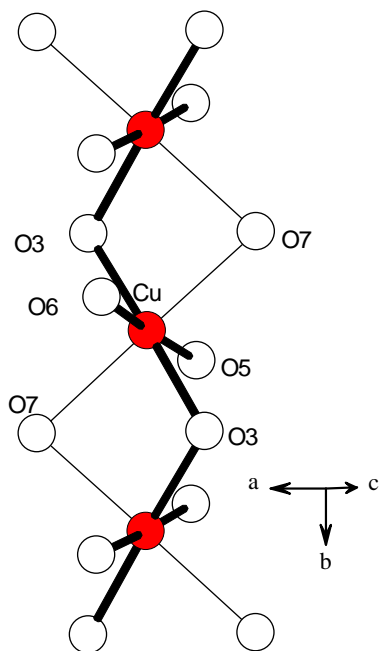


Fig. 6. Section of a Cu–O chain in **1**. The stretched Cu–O bonds are shown in thin lines.

stretched bonds and is nearly normal to the equatorial plane. The $d_{x^2-y^2}$ orbital has zero overlap with the O(7) p_σ orbital. The other bridge, O(3), is 3-coordinate with a nearly trigonal planar geometry. The mean deviation from the least-squares plane of O(3), P(1) and two Cu atoms is 0.016 Å. The magnetic orbitals on neighboring Cu ions form σ -type bonds with different sp^2 orbitals on the ligand. Because the spin correlation within a ligand always favors parallel alignment of the spins in orthogonal sp^2 orbitals, superexchange coupling via O(3) leads to a ferromagnetic interaction between Cu ions.

3.3. Discussion

In summary, we have synthesized a mixed metal phosphate incorporating isonicotinate ligand. It is the second example in the metal–isonicotinate–phosphate system. The structure consists of neutral sheet of $\text{CuVO}_2(\text{PO}_4)$ with the dipolar isonicotinate ligand being coordinated to two Cu^{II} cations as a pendent group. Each sheet is constructed from infinite chains of edge-sharing CuO_6 octahedra which are connected by double chains of vanadyl(V) phosphate. Magnetic study of **1** shows the presence of intrachain ferromagnetic coupling between Cu^{II} ions. The intrachain interaction is mainly through the Cu–O(3)–Cu–O(3) exchange pathway.

Recent studies have shown that isonicotinate ligand is able to bind metal centers with both pyridyl and carboxylate groups to form three-dimensional coordination polymers, where carboxylate groups balance the metal charges. In the structure of $\text{Zn}(\text{HINT})(\text{HPO}_4)$ the HPO_4^{2-} group balances the metal charge and the isonicotinate ligand binds the metal center with the carboxylate group only. In the title compound the total charge of Cu and VO_2 ions is balanced by PO_4^{3-} group. In order for isonicotinate to coordinate to metal centers with both the neutral and anionic groups, one may introduce a counter cation in the structure. Compounds with many possible compositions of anionic sub-lattice and different counter cations can be envisaged. Further research to synthesize open-framework materials in the M/INT/PO system by including appropriate organic amine templates in their structures is currently underway.

Acknowledgments

We thank the National Science Council for support, Ms. F.-L. Liao and Prof. S.-L. Wang at the National Tsing Hua University for X-ray data collection.

References

- [1] (a) H.-M. Lin, K.-H. Lii, Y.-C. Jiang, S.-L. Wang, *Chem. Mater.* 11 (1999) 519;
- (b) C.-Y. Chen, P.P. Chu, K.-H. Lii, *Chem. Commun.* 16 (1999) 1473;
- (c) Z.A.D. Lethbridge, P. Lightfoot, *J. Solid State Chem.* 143 (1999) 58;
- (d) Z.A.D. Lethbridge, A.D. Hiller, R. Cywinski, P. Lightfoot, *J. Chem. Soc. Dalton Trans.* 10 (2000) 1595;
- (e) A. Choudhury, S. Natarajan, C.N.R. Rao, *J. Solid State Chem.* 146 (1999) 538;
- (f) A. Choudhury, S. Natarajan, C.N.R. Rao, *Chem. Eur. J.* 6 (2000) 1168;
- (g) Y.-C. Jiang, S.-L. Wang, K.-H. Lii, N. Nguyen, A. Ducouret, *Chem. Mater.* 15 (2003) 1633 and references therein.

- [2] (a) K.-H. Lii, Y.-F. Huang, *Inorg. Chem.* 38 (1999) 1348;
(b) C.-Y. Chen, F.-R. Lo, H.-M. Kao, K.-H. Lii, *Chem. Commun.* 12 (2000) 1061;
(c) Y.-C. Jiang, Y.-C. Lai, S.-L. Wang, K.-H. Lii, *Inorg. Chem.* 40 (2001) 5320;
(d) L.-H. Huang, H.-M. Kao, K.-H. Lii, *Inorg. Chem.* 41 (2002) 2936;
(e) Z. Shi, S. Feng, S. Gao, L. Zhang, G. Yang, J. Hua, *Angew. Chem. Int. Ed.* 39 (2000) 2325;
(f) Z. Shi, S. Feng, L. Zhang, G. Yang, J. Hua, *Chem. Mater.* 12 (2000) 2930.
- [3] O.R. Evans, R.-G. Xiong, Z. Wang, G.K. Wong, W. Lin, *Angew. Chem. Int. Ed.* 38 (1999) 536.
- [4] J.Y. Lu, A.M. Babb, *Chem. Commun.* 9 (2001) 821.
- [5] C.-M. Wang, S.-T. Chuang, Y.-L. Chuang, H.-M. Kao, K.-H. Lii, *J. Solid State Chem.* 177 (2004) 1252.
- [6] G.M. Sheldrick, *SHELXTL Programs*, Version 5.1, Bruker AXS GmbH: Karlsruhe, Germany, 1998.
- [7] P.W. Selwood, *Magnetochemistry*, Interscience, New York, 1956.
- [8] I.D. Brown, D. Altermatt, *Acta Crystallogr. B* 41 (1985) 244.
- [9] X.-M. Zhang, H.-S. Wu, S. Gao, X.-M. Chen, *J. Solid State Chem.* 176 (2003) 69 and references therein.
- [10] G.A. Baker Jr., G.S.J. Rushbrooke, H.E. Gillbert, *Phys. Rev.* 135 (1964) A1272.
- [11] T. Ise, T. Ishida, D. Hashizume, F. Iwasaki, T. Nogami, *Inorg. Chem.* 42 (2003) 6106.